MOLECULAR AND CELLULAR BIOLOGY, Dec. 1995, p. 6838–6844 Vol. 15, No. 12
0270-7306/95/$04.00+0

Checkpoint Genes Required To Delay Cell Division in Response to Nocodazole Respond to Impaired Kinetochore Function in the Yeast *Saccharomyces cerevisiae*

YANCHANG WANG AND DANIEL J. BURKE*

Department of Biology, University of Virginia, Charlottesville, Virginia 22903

Received 27 June 1995/Returned for modification 15 August 1995/Accepted 7 September 1995

Inhibition of mitosis by antimitotic drugs is thought to occur by destruction of microtubules, causing cells to arrest through the action of one or more mitotic checkpoints. We have patterned experiments in the yeast *Saccharomyces cerevisiae* after recent studies in mammalian cells that demonstrate the effectiveness of antimitotic drugs at concentrations that maintain spindle structure. We show that low concentrations of nocodazole delay cell division under the control of the previously identified mitotic checkpoint genes *BUB1*, *BUB3*, *MAD1*, and *MAD2* and independently of *BUB2*. The same genes mediate the cell cycle delay induced in *ctf13* mutants, limited for an essential kinetochore component. Our data suggest that a low concentration of nocodazole induces a cell cycle delay through checkpoint control that is sensitive to impaired kinetochore function. The *BUB2* gene may be part of a separate checkpoint that responds to abnormal spindle structure.

Classic studies on the action of antimitotic drugs such as vinblastine and nocodazole interpreted the metaphase arrest as a consequence of unpolymerized microtubules and disrupted spindle structure (6, 27). However, recent studies showed that low concentrations of these drugs inhibited mitosis in HeLa cells with little or no depolymerization of spindle microtubules. Chromosomes were often detached from the spindle or had a monopolar orientation (17). Cells treated with low concentrations of vinblastine were analyzed by electron microscopy and had morphologically normal spindles with reduced numbers of kinetochore microtubules (39). Low concentrations of antimitotic drugs also suppressed microtubule dynamics in vitro (37). The authors concluded that the antimitotic effect of the drugs is due to suppression of microtubule dynamics necessary to establish bipolar chromosome attachments (17). They proposed that cells treated with low concentrations of antimitotic drugs do not attach kinetochores to the spindle and that the inability to make such attachments is responsible for arresting cell division (39).

Many cells have a checkpoint that arrests cells until all chromosomes attach to the spindle (25, 40), and the kinetochore appears to have an active role in checkpoint control (8, 33, 36, 38). Recent evidence suggests that a checkpoint inhibits anaphase until bipolar attachments between all kinetochores and the poles are achieved (28). The checkpoint-dependent arrest induced by a single unattached chromosome in insect cells can be overcome by applying tension on the kinetochore of the unattached chromosome (25). There is a phosphorylated epitope at the kinetochore in several cell types that may be involved in sensing or generating the signal required for arresting the cell cycle (10).

The structure and function of centromeres in the yeast *Saccharomyces cerevisiae* have been studied extensively. The minimal centromere DNA contains a 125-bp sequence organized into three domains, termed CDEI, CDEII, and CDEIII (5). CDEIII is an essential, imperfect palindrome, and point mutations in CDEIII completely inactive the centromere in vivo (11, 26). A protein complex termed CBF3 that binds tightly to CDEIII synthetic oligonucleotides has been purified by DNA affinity chromatography (23). CBF3 is primarily a 240-kDa multisubunit protein complex that contains three protein components, CBF3A, CBF3B, and CBF3C, plus some additional uncharacterized proteins (23). CBF3 binds to CDEIII throughout the cell cycle and binds to additional factors that mediate the interaction between CDEIII/CBF3 and microtubules in vitro (13, 31). The genes that encode the proteins in the 240-kDa complex have been cloned (7, 9, 15, 22, 34). CBF3A is essential for growth, and the structural gene was identified independently as *CBF2*/*NDC10*/*CTF14* (7, 9, 15). Temperature-sensitive *ndc10* mutants complete nuclear division at the restrictive temperature, but the chromosomes segregate asymmetrically. CTF3C is encoded by *CTF13*, and temperature-sensitive *ctf13* mutants delay at G_2/M in the cell cycle when grown at the restrictive temperature (32). CBF3B, the product of *CBF3*/*CEP3*, is a predicted zinc finger protein, and temperature-sensitive mutations result in cells that exhibit a G_2/M cell cycle delay (22, 34).

The yeast *S. cerevisiae* is sensitive to antimitotic benzimidazole drugs such as benomyl and nocodazole (14). High concentrations of the drug cause haploid cells to arrest cell division with unassembled microtubules, a 2*N* content of DNA, and undivided nuclei. Several mutants that are unable to delay the cell cycle in response to benzimidazoles have been isolated (12, 24). The mutants were isolated as benomyl-sensitive mutants that fail to arrest when grown in the presence of the drug. *bub* mutants (budding uninhibited by benzimidazoles) continue to bud and lose viability rapidly after treatment with high doses of benzimidazoles, and *mad* mutants (mitotic arrest deficient) are sensitive to lower, sublethal concentrations of benomyl.

The effects of high concentrations of benzimidazoles are not restricted to the mitotic spindle in yeast cells. Nuclear and cytoplasmic microtubules depolymerize in response to the drug, nuclear migration and positioning are affected, and nuclear structure is altered (14). Recent evidence from higher eucaryotic cells suggests that the mitotic (spindle) checkpoint is complex and is not restricted to impaired kinetochore function. The assembly state of the mitotic spindle, independent of kinetochore attachments, can influence the metaphase-an-

* Corresponding author. Phone: (804) 982-5482. Fax: (804) 982-4834. Electronic mail address: djb6t@virginia.edu.

TABLE 1. Yeast strains used in this study

Strain	Relevant genotype	Source
5943-1	*MAT***a** *ade5 can1 cyh2 leu2 lys5 ura3*	Burke laboratory
1130-1	*MAT***a** *ade2 bub1-1 can1 cyh2 ura3*	Burke laboratory
MAY2052	*MAT*α *lys2 his3 leu2 ura3 bub2::URA3*	M. A. Hoyt
MAY2074	*MAT*α *lys2 his3 leu2 ura3 bub3::LEU2*	M. A. Hoyt
DRL101-1C	*MAT***a** *his3 leu2 trp1 ura3 mad1-1*	A. Murray
DRL100-1D	*MAT***a** *his3 leu2 trp1 ura3 mad2-1*	A. Murray
YPH280R	*MAT***a** *ade2 his3 leu2 lys2 ura3 trp1 ctf13-30*	P. Hieter
1607-2-2	*MAT***a** *leu2 lys2 ura3 bub1-1 ctf13-30*	This study
795-5-2	*MAT*α *his3 leu2 lys2 ura3 bub2::URA3 ctf13-30*	This study
794-9-4	*MAT*α *his3 leu2 lys2 trp1 ura3 bub3::LEU2 ctf13-30*	This study
793-7-4	*MAT*α *ade2 his3 leu2 trp1 ura3 mad1-1 ctf13-30*	This study
792-1-1	*MAT***a** *ade2 his3 leu2 trp1 ura3 mad2-1 ctf13-30*	This study

aphase transitions (2, 3). It is conceivable that the spindle checkpoint in yeast cells, defined by the *MAD* and *BUB* genes, responds to complex physiological perturbations, given the potentially large number of cellular processes that are affected by nocodazole.

In this study, we identify a low concentration of nocodazole that causes haploid cells to delay cell division with a 2*N* content of DNA and undivided nuclei. Treated cells are viable, and microtubule spindle structure is not detectably affected, as determined by indirect immunofluorescence with antitubulin staining. *BUB1*, *BUB3*, *MAD1*, and *MAD2* are required for cells to maintain viability when treated with the low concentration of nocodazole. *BUB2* is not required for maintaining viability. All of the checkpoint genes are required to maintain viability of cells that are treated with a higher concentration of nocodazole that destroys microtubule structure. We have compared the aforementioned response of the checkpoint mutants with the cell cycle delay induced in *ctf13* mutants limited for an essential kinetochore component. We show that the delay in a *ctf13* mutant requires *BUB1*, *BUB3*, *MAD1*, and *MAD2* and is independent of *BUB2*. Our data suggest that the low concentration of nocodazole induces a cell cycle delay through a checkpoint control that is kinetochore dependent. The checkpoint genes *BUB1*, *BUB3*, *MAD1*, and *MAD2* respond to impaired kinetochore function, whereas *BUB2* may respond to abnormal spindle structure.

MATERIALS AND METHODS

Yeast strains, growth, and media. The genotypes and sources of relevant *S. cerevisiae* strains used in this work are listed in Table 1. Strains were constructed by standard genetic methods (30). YM-1 and YEPD are rich media and were used as described before (4, 30). Nocodazole (Sigma) was added to medium containing 1% dimethyly sulfoxide as described previously (14). Cell counts were performed by microscopy with the aid of a hemacytometer after clumped cells were disrupted by sonication. Plating efficiency was determined by direct observation of cells that were spread on YEPD plates. Viable cells formed microcolonies, visible after 12 h, on the surface of the plates. Inviable cells divided, at most, two times.

Indirect immunofluorescence. Immunofluorescence and DNA staining with 4′,6-diamidino-2-phenylindole (DAPI) were done as described previously (1). The monoclonal rat antitubulin antibody YOL1/34 and secondary (fluorescein isothiocyanate derivatized) goat anti-rat antibody (Seralabs) were diluted 1:50 with phosphate-buffered saline (PBS) containing 1% bovine serum albumin. Cells were viewed with a Zeiss IM 35 microscope equipped with a neoflaur lens (N.A. 1.4) and photographed with a Photometrics cooled charge-coupled device camera equipped with a KAF 1400 chip (Kodak). Images were acquired with PMIS (Photometrics) and stored as eight-bit TIFF files and analyzed with MOCHA (Jandel Scientific). Fluorescence measurements were calibrated by using commercial standards (Molecular Probes), and all measurements were within the linear range of the camera. The lengths of spindles were calculated from images obtained with MOCHA according to the manufacturer's instructions. Photographs were prepared from the TIFF files by using Photoshop (Adobe) and labeled and printed with a Codonics 600 dye sublimation printer.

Flow cytometry. The DNA content of cells was determined by flow cytometry of propidium iodide-stained cells as described previously (4). Flow cytometric profiles were quantified by using SIGMAPLOT (Jandel Scientific), assuming Gaussian distributions in the G_1 and G_2/M peaks.

RESULTS

Low concentrations of nocodazole delay the yeast cell cycle. Yeast cells treated with high concentrations of nocodazole respond by rapidly depolymerizing microtubules and arresting cell division after DNA synthesis, before nuclear division (14). Jordan et al. (17) showed that the lowest effective concentration of nocodazole arrests HeLa cells with a fully assembled mitotic spindle. To determine if there was a low concentration of nocodazole that had a similar effect on yeast cells, we determined the rate of cell division of wild-type strain 5943-1 in medium containing increasing amounts of nocodazole at 30°C. Nocodazole affected cell division at concentrations above 3 μg/ml (Fig. 1). Cells treated with 3 μg of nocodazole per ml divided at a rate that was 77% of that of untreated cells.

We stained treated cells with propidium iodide and determined the DNA content of individual cells by flow cytometry. Cells that were untreated had two peaks in the DNA profiles, with approximately 61% of the cells having a 2*N* content of DNA (Fig. 2A). Cells treated with 3 μg of nocodazole per ml were larger, and approximately 78% of the cells had a 2*N* content of DNA (Fig. 2B). To determine if microtubules were present in cells treated with 3 μg of nocodazole per ml, we fixed treated and untreated cells with formaldehyde. We visualized microtubules by indirect immunofluorescence with an antitubulin antibody and visualized DNA by using DAPI. The data (Fig. 3) show that spindles were present in the nuclei of

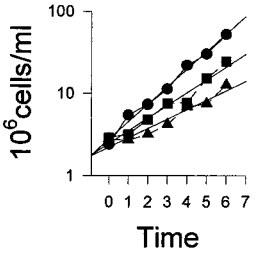

FIG. 1. Growth rates in various concentrations of nocodazole. Cells were inoculated into YM-1 medium at a density of 3×10^6 cells per ml and grown at 30°C for the indicated times (hours). Cell number was determined by counting with a hemacytometer. Each point is the average of two independent counts of more than 200 cells. Data were plotted by using Sigmaplot (Jandel Scientific), and linear regressions are included. Nocodazole concentrations: ●, 0 μg/ml; ■, 3 μg/ml; ▲, 4 μg/ml.

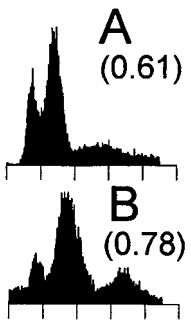

FIG. 2. Flow cytometry of cells after growth in 3 μg of nocodazole per ml. Cells were grown for 4 h in YM-1 containing no nocodazole (A) or 3 μg of nocodazole per ml (B), fixed with ethanol, and stained with propidium iodide. The fraction of cells in G_2/M is indicated in parentheses.

cells treated with nocodazole. Of the untreated cells, 19% (n = 200) had a short spindle and an undivided nucleus positioned at the isthmus between the mother cell and the bud. In contrast, 42% (n = 200) of the treated cells had a similar morphology. The majority of the other cells had microtubule structures, including spindles, that were indistinguishable in structure from those of wild-type cells. All of the structures that can be recognized in untreated cells (20) were also present in cells grown in 3 μg of nocodazole per ml. The intensity of fluorescence staining in cells with spindles 1 to 2 μm long was determined from digital images by using the MOCHA (Jandel Scientific) image analysis software. Fluorescence intensity was similar between treated and untreated cells. We conclude that 3 μg of nocodazole per ml affects cell division in yeast cells without markedly depolymerizing microtubules. Treated cells delayed in the cell cycle after DNA synthesis and prior to nuclear division. Cells had mitotic spindles that were similar in structure to those of untreated wild-type cells at the same stage of the cell cycle.

Nocodazole effects on cell division require some mitotic checkpoint genes. Mitotic checkpoint mutants (*mad* and *bub* mutants) were previously identified as benomyl-sensitive mutants that failed to arrest in the cell cycle after growth in high concentrations of benomyl (12, 24). The high concentrations of benomyl used to isolate the *bub* mutants (70 μg/ml) resulted in nearly complete loss of microtubule structure (12). The lower concentration of benomyl used to isolate *mad* mutants (15 μg/ml) caused cells to grow slowly, at 0.41 times the rate of wild-type cells (24). This rate is comparable to that of our wild-type cells grown in medium containing 6 μg of nocodazole per ml. We analyzed our wild-type cells, grown in medium containing 6 μg of nocodazole per ml, by indirect immunofluorescence with antitubulin antibodies. Of the 200 cells, 62% had few or greatly diminished microtubule structures in the cell. We conclude that both the *bub* and *mad* mutants were isolated under conditions that dramatically affect microtubule and spindle structure in wild-type cells.

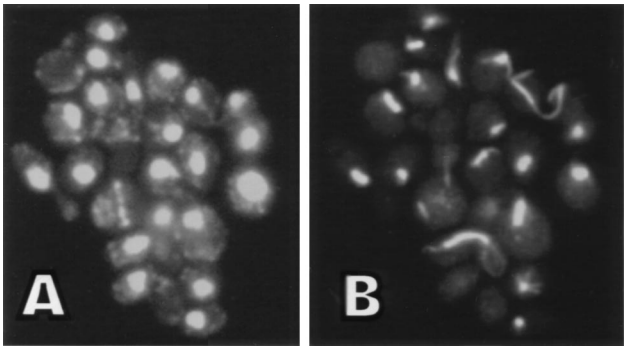

FIG. 3. Cytological analysis of cells treated with nocodazole (3 μg/ml). Wild-type cells were grown in medium containing 3 μg of nocodazole per ml for 4 h at 30°C, fixed with formaldehyde, and stained with DAPI (A) or with YOL1/34, an antitubulin antibody (B).

TABLE 2. Plating efficiency after growth for 5 h in medium containing nocodazole

Strain	Mean plating efficiency (SEM) at nocodazole concn of:		
	0 μg/ml	3 μg/ml	8 μg/ml
5943-1 (wild type)	98.7 (1.2)	94.3 (2.3)	54.7 (3.5)
1130-1 (*bub1-1*)	93.0 (1.4)	25.5 (4.9)	0.5 (0.7)
MAY2052 (*bub2*::*URA3*)	98.0 (1.0)	85.3 (4.0)	9.7 (3.2)
MAY2074 (*bub3*::*LEU2*)	84.3 (6.7)	26.0 (15.7)	0.7 (1.2)
DRL101-1C (*mad1-1*)	96.3 (1.5)	64.3 (13.8)	5.3 (4.5)
DRL100-1D (*mad2-1*)	95.3 (2.5)	18.3 (2.5)	1.3 (0.6)

To determine if the mitotic checkpoint mutants were sensitive to the low concentration of nocodazole, we compared the plating efficiency of checkpoint mutants and a wild-type strain after growth in medium containing two concentrations of the drug (Table 2). The lowest concentration (3 μg/ml) did not detectably affect microtubule structures, and the higher concentration (8 μg/ml) caused wild-type cells to arrest cell division with greatly diminished antitubulin staining, as described previously (14). The wild-type strain and the *bub2* mutant retained high viability in 3 μg of nocodazole per ml. The viability of the *mad1* mutant strain was moderately affected by growth in 3 μg of nocodazole per ml, and the *mad2*, *bub1*, and *bub3* mutant strains were dramatically affected. The plating efficiency was affected in all of the mutants when grown in medium containing 8 μg of nocodazole per ml. These data suggest that the mutants can be divided into two groups. One group (including the *mad1*, *mad2*, *bub1*, and *bub3* mutants) is either moderately or dramatically affected by 3 μg of nocodazole per ml, and the other group (*bub2* mutants) is unaffected by this low concentration of the drug.

To determine if the low concentration of nocodazole affected the ability of checkpoint mutants to delay cell division, we compared the morphologies of cells treated with 3 μg of nocodazole per ml. Wild-type cells grown in the presence of the drug had an increased percentage of cells with large buds and a single undivided nucleus (Table 3), which we interpret as indicative of the delay induced in the cell cycle by nocodazole. The *bub2* mutant delayed cell division in response to nocodazole, but the other checkpoint mutants did not. We infer that the inviability of checkpoint mutants treated with nocodazole is due to the inability to delay the cell cycle. We conclude that *MAD1*, *MAD2*, *BUB1*, and *BUB3* are required to delay cell division in response to nocodazole at 3 μg/ml.

***MAD* and *BUB* genes respond to defective kinetochores.** Our data suggest that some checkpoint genes can signal a cell cycle delay in response to nocodazole when apparently normal spindle structures are present in the cell. Therefore, the mitotic spindle checkpoint can be activated by nocodazole under conditions that do not eliminate nuclear and cytoplasmic microtubules and when the nucleus is not displaced. This suggests that there must be some perturbation, other than microtubule depolymerization, utilized by the spindle checkpoint that can signal a delay. One intriguing possibility is provided by the

TABLE 3. Percentage of cycling cells that were large budded after growth in the presence or absence of nocodazole[a]

Strain	Mean % large-budded cells (SEM) at nocodazole concn of:			
	Undivided		Divided	
	0 μg/ml	3 μg/ml	0 μg/ml	3 μg/ml
5943-1 (wild type)	23.7 (4.0)	50.0 (4.6)	28.0 (4.0)	24.0 (3.5)
DRL101-1C (*mad1*)	12.7 (2.5)	16.0 (2.0)	19.7 (9.0)	36.7 (6.5)
DRL100-1D (*mad2*)	18 (3.5)	18.0 (5.0)	29.7 (8.1)	28.3 (6.4)
1130-1 (*bub1*)	18.0 (2.6)	19.0 (5.3)	29.7 (1.2)	25.3 (1.5)
MAY2052 (*bub2*)	14.0 (2.6)	32.2 (5.3)	32.3 (7.3)	23.3 (7.6)
MAY2074 (*bub3*)	18.3 (3.5)	23.3 (5.9)	35.7 (7.6)	30.7 (7.4)

[a] Large-budded cells had a bud size greater than 50% of the mother cell size. Undivided cells had a single DAPI-staining body. Divided cells had two separate DAPI-staining bodies. All percentages were determined from three independent experiments, each counting greater than 200 cells.

experiments with mammalian cells that suggest that antimitotic drugs affect cell division by interfering with kinetochore attachments to the spindle (17, 39). We cannot visualize centromere-microtubule attachments by direct cytological observations in yeast cells to determine if kinetochores are attached to microtubules when cells are grown in low concentrations of nocodazole. However, we can determine if cells will delay when kinetochore function is compromised by using a mutation in *CTF13*, a gene that encodes an essential kinetochore component (7). If the low concentration of nocodazole inhibits cell division by interfering with kinetochore function, then the mitotic checkpoint genes should be required for arresting cell division in *ctf13* mutants.

Haploid, temperature-sensitive *ctf13* mutants, when incubated at 37°C, arrest in the cell cycle with a short spindle and an undivided nucleus (7). *ctf13* mutants grow slowly at 32°C (a semipermissive temperature), presumably because they have a limited amount of functional Ctf13p. We constructed *ctf13* mutants with additional *mad1*, *mad2*, *bub1*, *bub2*, or *bub3* mutations and incubated serial 10-fold dilutions of the mutants at 23°C, the permissive temperature for *ctf13*, and at 32°C. The data (Fig. 4) show that *ctf13* (row A) and *ctf13 bub2* (row C) mutants grew at both temperatures but that all other double mutants grew poorly at the semipermissive temperature. None of the *mad* and *bub* single mutants were temperature sensitive, as growth was unaffected at 32°C.

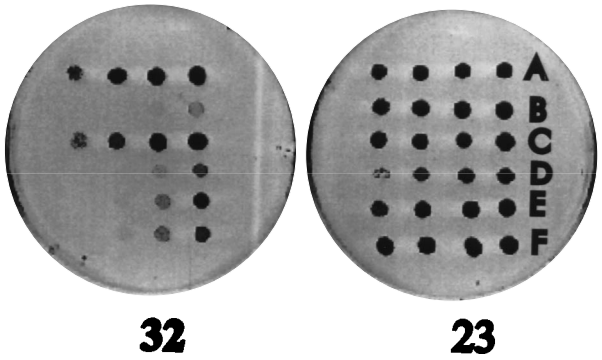

FIG. 4. Growth of *ctf13* single and double mutants limited for *CTF13* function. Cells were grown in YM-1 at the permissive temperature of 23°C, and serial 10-fold dilutions (from right to left) were spotted onto YEPD plates and incubated at the indicated temperature of 23 or 32°C. (A) *ctf13*; (B) *ctf13 bub1*; (C) *ctf13 bub2*; (D) *ctf13 bub3*; (E) *ctf13 mad1*; (F) *ctf13 mad2.*

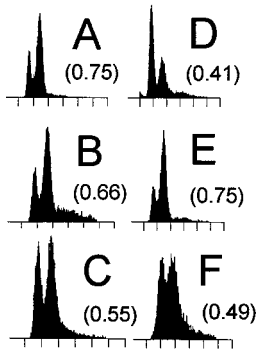

FIG. 5. Flow cytometry of *ctf13* single and double mutants after growth at the restrictive temperature. Cells were grown to a density of 3×10^6 cells per ml in YM-1 medium, incubated at 38°C for 3 h, fixed with ethanol, and stained with propidium iodide. (A) *ctf13*; (B) *ctf13 mad1*; (C) *ctf13 mad2*; (D) *ctf13 bub1*; (E) *ctf13 bub2*; (F) *ctf13 bub3*. The fraction of cells in G_2/M is indicated in parentheses.

We also determined the plating efficiency for the *ctf13* and double mutant strains after growth at the restrictive temperature. The data (Table 4) show that the double mutants with *ctf13* and *mad2*, *bub1*, or *bub3* mutations were inviable after short incubations at the restrictive temperature compared with the *ctf13* mutant. The viability of the *ctf13 mad1* double mutant was also reduced after short incubations at the restrictive temperature, but the effect was less dramatic. The *ctf13 bub2* double mutant was only slightly affected by short incubations at the restrictive temperature. In each case, the inviability was due to the *ctf13* mutation. The plating efficiency of the *bub1* mutant (strain 1130-1) after 3 h of growth at 38°C was 0.71. All of the other checkpoint mutants were modestly affected by 3 h of growth at 38°C, and plating efficiencies were greater than 0.80. We infer that the mitotic checkpoint genes *MAD1*, *MAD2*, *BUB1*, and *BUB3* are required to arrest cell division when cells are limited for *CTF13* function.

To determine if the enhanced temperature sensitivity of *ctf13* double mutants with mitotic checkpoint mutations resulted from bypass of the arrest in the cell cycle, we analyzed the proportion of cells at different stages of the cell cycle after incubating *ctf13* mutant cells and the double mutants at the restrictive temperature and analyzed the DNA content of cells by flow cytometry. We found that a larger percentage of *ctf13* mutant cells (63%) arrested as large budded cells with short spindles when the temperature was increased to 38°C, and therefore we used this as the restrictive temperature. The data for the *ctf13* mutants were very similar to the published results (7), and approximately 75% of the cells had the G_2/M content of DNA. The DNA profiles were similar for the *ctf13* mutant (Fig. 5A) and *ctf13 bub2* double mutants (75% G_2/M) (Fig. 5E). The DNA profiles were slightly different for the *ctf13 mad1* double mutant (66% G_2/M) (Fig. 5B). The other double mutants had a smaller proportion of cells with a 2*N* content of DNA, suggesting that they were unable to maintain the arrest in the cell cycle. We also compared spindle staining by indirect immunofluorescence with an antitubulin antibody in a *ctf13* mutant and in the double mutants. The data show that most *ctf13* mutant cells (Fig. 6A and D) and *ctf13 bub2* mutant cells (Fig. 6B and E) were arrested with a short spindle and an undivided nucleus. In contrast, cells of the *ctf13 mad1* double mutant (Fig. 6C and F) were unable to maintain the arrest and had a reduced percentage of cells with a short spindle. Similar results were obtained for the *ctf13* and *mad2*, *bub1*, and *bub3*

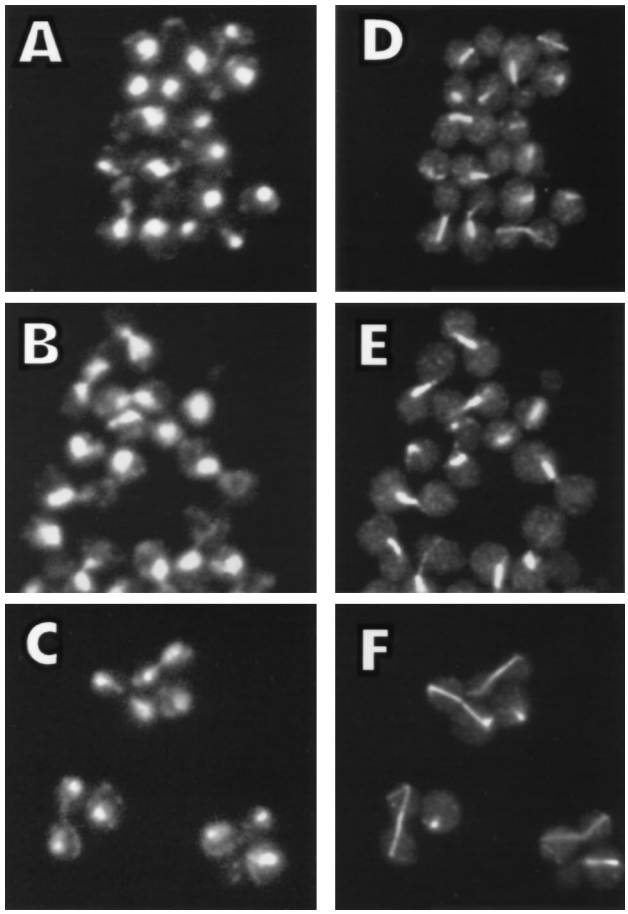

FIG. 6. Cytological analysis of *ctf13* single and double mutants. Cells were grown to a density of 10^6 cells per ml in YM-1 medium at 23°C, incubated at 38°C for 3 h, fixed with formaldehyde, and stained with DAPI (A to C) or with YOL1/34, an antitubulin antibody (D to F). (A and D) *ctf13*; (B and E) *ctf13 bub2*; (C and F) *ctf13 mad1.*

double mutants (Table 4). In addition, there were an unusually high proportion of cells from the *ctf13 mad1* double mutant (15%) that were large budded with divided nuclei that contained a single spot of tubulin staining in each nucleus. The proportion of these cells was not affected by repeated sonication of the cells prior to fixation or to prolonged zymolyase treatment after fixation. We conclude that the *ctf13 mad1* double mutant could not maintain the medial nuclear division delay. Cells completed nuclear division but not cytokinesis and therefore appeared in flow cytometric DNA profiles as cells with a 2*N* content of DNA. Our data suggest that *ctf13* mutants grown at the restrictive temperature delay in the cell cycle through the action of the *BUB1*, *BUB3*, *MAD1*, and *MAD2* genes.

DISCUSSION

Haploid *S. cerevisiae* cells delayed cell division when grown in the presence of 3 μg of nocodazole per ml. Flow cytometry and indirect immunofluorescence were used to show that cells delay after DNA synthesis, prior to nuclear division, with apparently intact mitotic spindle structures. The mitotic checkpoint genes *BUB1*, *BUB3*, *MAD1*, and *MAD2* were required to delay the cell cycle, but *BUB2* was not required. In addition, we showed that the cell cycle delay in *ctf13* mutants required the same checkpoint genes, *BUB1*, *BUB3*, *MAD1*, and *MAD2*, and was independent of *BUB2*. Our data suggest that the lowest effective concentration of nocodazole induces a cell cycle delay mediated through the same checkpoint genes.

Antimitotic drugs have been widely used as chemotherapeutic agents in treating cancer (29) and as molecular probes in understanding microtubule functions in living cells that are not amenable to classic genetic analysis (3, 16–18, 39). The theory that cells arrest when microtubules are completely destroyed has been reevaluated in recent studies and has led to a more sophisticated view of how these drugs interfere with microtubule function in vivo and in vitro (16–19, 39). Their seminal discovery is that the drugs affect cell division at concentrations that do not completely destroy microtubule and spindle structure. They propose that the primary effect of the drug is to inhibit microtubule dynamics, which prevents chromosome attachment to the spindle. The unattached chromosome then signals a cell cycle arrest, which accounts for the antiproliferative properties of the drug (17).

We were interested in testing these ideas in the yeast *S. cerevisiae*. The simple organization of tubulin genes in this organism coupled with the facile methods for manipulating the genes should make the organism invaluable for studying the pharmacological effects of the drugs in addition to various aspects of microtubule structure, function, and regulation. The wealth of genetic data on the DNA and protein components of the centromere as well as potential regulators of the spindle checkpoint that already exist allows us to compare the effects of nocodazole with those of mutations that affect kinetochore function, independent of other spindle perturbations (12, 23, 24).

S. cerevisiae cells grown in the presence of 3 μg of nocodazole per ml divided more slowly than untreated cells, without a noticeable change in microtubule structure. We calculate that 3 μg of nocodazole per ml increased the generation time by approximately 30%. The increased number of cells with a G_2/M content of DNA coupled with the increased number of cells with a short spindle and an undivided nucleus suggests that the cells spend the extra time in the cell cycle at mitosis. The delay in the cell cycle induced by nocodazole required the mitotic checkpoint genes *BUB1*, *BUB3*, *MAD1*, and *MAD2*. These data suggest that the spindle checkpoint responds to a limited subset of the physiological perturbations that occur in nocodazole-treated cells.

Mutations that weaken a single centromere and mutations in genes that encode centromere DNA-binding proteins can delay the cell cycle in *S. cerevisiae*, suggesting a role for the kinetochore in checkpoint control in yeast cells (7, 33). A

TABLE 4. Comparison of wild-type and *ctf13* mutants after incubation for 3 h at 38°C

Strain	% of cells with[a]:		No. of cells examined	Mean plating efficiency (SEM)
	Short spindle	Long spindle		
5943-1 (wild type)	19.4	14.1	284	0.93 (0.08)
YPH280R (*ctf13*)	63.1	6.7	312	0.81 (0.07)
1607-2-2 (*ctf13 bub1*)	10.5	5.3	228	0.11 (0.09)
795-5-2 (*ctf13 bub2*)	66.1	9.1	372	0.73 (0.10)
794-9-4 (*ctf13 bub3*)	14.2	11.9	253	0.25 (0.11)
793-7-4 (*ctf13 mad1*)	19.7	22.6	239	0.50 (0.22)
792-1-1 (*ctf13 mad2*)	8.3	14.8	277	0.35 (0.13)

[a] Spindle length was determined after antitubulin staining. Short, shorter than 5 μm; long, longer than 5 μm.

temperature-sensitive mutation in *CTF13* (*ctf13-30*), a component of the protein complex that binds centromeric DNA and facilitates microtubule binding to centromere DNA, dramatically affects chromosome segregation (7). *ctf13* mutants grown at 37°C delay at mitosis but eventually continue to anaphase, suggesting that impaired kinetochore function induces a cell cycle delay. We found that *BUB1*, *BUB3*, *MAD1*, and *MAD2* are required for the delay that results from reduced *CTF13* function. We conclude that these genes are part of the mitotic checkpoint that arrests cells when kinetochore function is compromised.

Ctf13p is required for binding centromere DNA to microtubules in vitro, and extracts prepared from *ctf13* mutant cells are completely devoid of microtubule-binding activity (31). Kinetochore-microtubule interactions cannot be directly visualized in yeast cells, and therefore it is not currently possible to determine if centromeres are attached to the spindle microtubules in *ctf13* mutants in vivo. Assuming that the in vitro assay is a true reflection of the in vivo function of Ctf13p, the cell cycle delay in *ctf13* mutants may result from an inhibitory signal produced by one or more unattached chromosomes. A checkpoint that delays cell division in response to unattached chromosomes has been described, and the kinetochore has been implicated in the signaling (10, 36, 40). We propose that *ctf13* mutants retain some, but not all, microtubule-binding activity in vivo and that *MAD1*, *MAD2*, *BUB1*, and *BUB3* are part of the checkpoint that can signal an arrest in the cell cycle when kinetochore-microtubule interactions are compromised. There are a sufficient number of centromeres that are unattached in *ctf13* mutants to signal a delay at 37°C. Increasing the temperature inactivates more Ctf13p, and a higher proportion of cells are arrested. Eliminating the cell cycle checkpoint by using *ctf13* and either *bub1*, *bub3*, *mad1*, or *mad2* double mutants forces cells with unattached chromosomes into anaphase, resulting in lethality. The same genes that are required for the cell cycle delay in response to the low concentration of nocodazole are also required for the delay when cells are limited for *CTF13* function. We infer that the antimitotic effect of nocodazole is primarily due to inhibition of microtubule-kinetochore interactions.

The *MAD1* gene is required to maintain the delay in response to the low concentration of nocodazole and when cells are limited for *CTF13* function. Therefore, we have included *MAD1* among the genes that respond to impaired kinetochore function. However, the phenotype of the *mad1* mutant in response to the spindle perturbations was different from those of the other checkpoint mutants. The *mad1* mutant retained higher viability than other checkpoint mutants when treated with nocodazole, and the *ctf13 mad1* double mutant strain retained some viability when incubated at the restrictive temperature. The *mad1-1* allele may have residual *MAD1* activity, and some of the cells may retain the checkpoint in the presence of nocodazole or when limited for *CTF13* function. Spindle elongation occurred in the *ctf13 mad1* double mutant incubated at the restrictive temperature, but the cells did not complete cell division and accumulated as large budded cells with divided nuclei. This may be part of a mechanism that prevents cytokinesis from occurring until the spindle checkpoint is inactivated, and residual activity in *mad1-1* mutants may be preventing cytokinesis. Alternatively, *MAD1* may have additional functions in the cell, in addition to the spindle checkpoint, resulting in phenotypes different from those of other checkpoint mutants.

The *BUB2* gene does not appear to have a role in the same checkpoint, although previous experiments suggest that it plays a role in mitotic regulation (12). *bub2* mutants were isolated as mutants supersensitive to high concentrations of nocodazole, and it is possible that the pleiotropic effects of the drug activate a different regulatory response. Recent data from this laboratory suggest that *BUB2* is required to maintain the arrest in temperature-sensitive *cdc20* mutants that arrest cell division with abnormal spindles (35). It is possible that *S. cerevisiae* has additional complexity in mitotic spindle checkpoint control, analogous to that suggested by experiments with higher eucaryotic cells (3, 21).

ACKNOWLEDGMENTS

This work was supported by N.I.H. grant GM 40334 and by support from Thomas F. Jeffress and Kate Miller Jeffress Memorial Trust grant J-288.

We thank Andy Hoyt, Phil Hieter, and Andrew Murray for providing strains. We also thank Mitch Smith for assistance with flow cytometry, Jay Hirsh for assistance with network printing, and Penny Tavormina for many useful discussions and for comments on the manuscript.

REFERENCES

1. **Adams, A. E. M., and J. R. Pringle.** 1984. Relationship of actin and tubulin distribution to bud growth in wild type and morphogenetic mutants of *Saccharomyces cerevisiae*. J. Cell Biol. **98:**934–945.
2. **Andreassen, P. R., and R. L. Margolis.** 1991. Induction of partial mitosis in BHK cells by 2-aminopurine. J. Cell Sci. **100:**299–310.
3. **Andreassen, P. R., and R. L. Margolis.** 1994. Microtubule dependence of p34(CDC2) inactivation and mitotic exit in mammalian cells. J. Cell Biol. **127:**789–802.
4. **Burke, D., P. Gasdaska, and L. Hartwell.** 1989. Dominant effects of tubulin overexpression in *Saccharomyces cerevisiae*. Mol. Cell. Biol. **9:**1049–1059.
5. **Cottarel, G., J. H. Shero, P. Hieter, and J. H. Hegemann.** 1989. A 125-base-pair *CEN6* DNA fragment is sufficient for complete meiotic and mitotic centromere functions in *Saccharomyces cerevisiae.* Mol. Cell. Biol. **9:**3342–3349.
6. **DeBrabander, M. J., R. M. L. Vande Veire, F. E. M. Aerts, M. Borgers, and P. A. J. Janssen.** 1976. The effect of methyl(5-(2-thienylcarbonyl)-1H-benzimidazole-2-yl)carbamate (R17934; NSC 238159), a new synthetic antitumoral drug interfering with microtubules on mammalian cells cultured *in vitro*. Cancer Res. **36:**905–916.
7. **Doheny, K. F., P. K. Sorger, A. A. Hyman, S. Tugendreich, F. Spencer, and P. Hieter.** 1993. Identification of essential components of the *S. cerevisiae* kinetochore. Cell **73:**761–774.
8. **Earnshaw, W. C., R. L. Bernat, C. A. Cooke, and N. F. Rothfield.** 1991. Role of the centromere/kinetochore in cell cycle control. Cold Spring Harbor Symp. Quant. Biol. **56:**675–685.
9. **Goh, P., and J. V. Kilmartin.** 1993. *NDC10*: a gene involved in chromosome segregation in *Saccharomyces cerevisiae*. J. Cell Biol. **121:**503–512.
10. **Gorbsky, G. J., and W. A. Ricketts.** 1993. Differential expression of a phosphoepitope at the kinetochores of moving chromosomes. J. Cell Biol. **122:** 1311–1321.
11. **Hegemann, J. H., J. H. Shero, G. Cottarel, P. Philippsen, and P. Hieter.** 1988. Mutational analysis of centromere DNA from chromosome VI of *Saccharomyces cerevisiae*. Mol. Cell. Biol. **8:**2523–2535.
12. **Hoyt, M. A., L. Totis, and B. T. Roberts.** 1991. *S. cerevisiae* genes required for cell cycle arrest in response to loss of microtubule function. Cell **66:**507–517.
13. **Hyman, A. A., K. Middleton, M. Centola, T. J. Mitchison, and J. Carbon.** 1992. Microtubule-motor activity of a yeast centromere-binding protein complex. Nature (London) **359:**533–536.
14. **Jacobs, C. W., A. E. M. Adams, P. J. Szaniszlo, and J. R. Pringle.** 1988. Functions of microtubules in the *Saccharomyces cerevisiae* cell cycle. J. Cell Biol. **107:**1409–1426.
15. **Jiang, W., J. Lecher, and J. Carbon.** 1993. Isolation and characterization of a gene (*CBF2*) specifying a protein component of the budding yeast kinetochore. J. Cell Biol. **121:**513–519.
16. **Jordan, M. A., D. Thrower, and L. Wilson.** 1991. Mechanism of inhibition of cell proliferation by vinca alkaloids. Cancer Res. **51:**2212–2222.
17. **Jordan, M. A., D. Thrower, and L. Wilson.** 1992. Effect of vinblastine, podophyllotoxin and nocodazole on mitotic spindles: implication for the rate of microtubule dynamics in mitosis. J. Cell Sci. **102:**401–416.
18. **Jordan, M. A., R. J. Toso, D. Thrower, and L. Wilson.** 1993. Mechanism of mitotic block and inhibition of cell proliferation by taxol at low concentrations. Proc. Natl. Acad. Sci. USA **90:**9552–9556.
19. **Jordan, M. A., and L. Wilson.** 1990. Kinetic analysis of tubulin exchange at microtubule ends at low vinblastine concentrations. Biochemistry **29:**2730–2739.
20. **Kilmartin, J. V., and A. E. Adams.** 1984. Structural rearrangements of tubulin and actin during the cell cycle of the yeast *Saccharomyces*. J. Cell Biol. **98:**922–933.

21. **Kubiak, J. Z., M. Weber, H. D. Pennart, N. J. Winston, and B. Maro.** 1993. The metaphase II arrest in mouse oocytes is controlled through microtubule-dependent destruction of cyclin B in the presence of CSF. EMBO J. **12:** 3773–3778.
22. **Lechner, J.** 1994. A zinc finger protein, essential for chromosome segregation, constitutes a putative DNA binding subunit of the *Saccharomyces cerevisiae* kinetochore complex Cbf3. EMBO J. **13:**5203–5211.
23. **Lechner, J., and J. Carbon.** 1991. A 240 kD multisubunit protein complex, CBF3, is a major component of the budding yeast centromere. Cell **64:**717–725.
24. **Li, R., and A. W. Murray.** 1991. Feedback control of mitosis in budding yeast. Cell **66:**519–531.
25. **Li, X., and R. B. Nicklas.** 1995. Mitotic forces control a cell-cycle checkpoint. Nature (London) **373:**630–632.
26. **Ng, R., and J. Carbon.** 1987. Mutational and in vitro protein-binding studies on centromere DNA from *Saccharomyces cerevisiae*. Mol. Cell. Biol. **7:**4522–4534.
27. **Owellen, R. J., C. A. Hartke, R. M. Dickerson, and F. O. Hains.** 1976. Inhibition of tubulin-microtubule polymerization by drugs of the vinca alkaloid class. Cancer Res. **36:**1499–1502.
28. **Rieder, C. L., A. Schultz, R. Cole, and G. Sluder.** 1994. Anaphase onset in vertebrate somatic cells is controlled by a checkpoint that monitors sister kinetochore attachment to the spindle. J. Cell Biol. **127:**1301–1310.
29. **Rowinsky, E. K., and R. C. Donehower.** 1991. The clinical pharmacology and use of antimicrotubule agents in cancer chemotherapeutics. Pharmacol. Ther. **52:**35–84.
30. **Sherman, F., G. Fink, and J. B. Hicks.** 1986. Methods in yeast genetics. Cold Spring Harbor Laboratory, Cold Spring Harbor, N.Y.
31. **Sorger, P. K., F. F. Severin, and A. A. Hyman.** 1994. Factors required for the binding of reassembled yeast kinetochores to microtubules *in vitro*. J. Cell Biol. **127:**995–1008.
32. **Spencer, F., S. L. Gerring, C. Connelly, and P. Hieter.** 1990. Mitotic chromosome transmission fidelity mutants in *Saccharomyces cerevisiae*. Genetics **124:**237–249.
33. **Spencer, F., and P. Hieter.** 1992. Centromere DNA mutations induce a mitotic delay in *Saccharomyces cerevisiae*. Proc. Natl. Acad. Sci. USA **89:** 8908–8912.
34. **Strunnikov, A. V., J. Kingsbury, and D. Koshland.** 1995. *CEP3* encodes a centromere protein of *Saccharomyces cerevisiae*. J. Cell Biol. **128:**749–760.
35. **Tavormina, P.** Personal communication.
36. **Tomkiel, J., C. A. Cooke, H. Saitoh, R. L. Bernat, and W. C. Earnshaw.** 1994. CENP-C is required for maintaining proper kinetochore size and for a timely transition to anaphase. J. Cell Biol. **125:**531–545.
37. **Toso, R. J., M. A. Jordan, K. W. Farrell, B. Matsumoto, and L. Wilson.** 1993. Kinetic stabilization of microtubule dynamic instability *in vitro* by vinblastine. Biochemistry **32:**1285–1293.
38. **Wang, X., N. Yew, J. G. Peloquin, G. F. Vandewoude, and G. G. Borisy.** 1994. Mos oncogene product associates with kinetochores in mammalian somatic cells and disrupts mitotic progression. Proc. Natl. Acad. Sci. USA **91:**8329–8333.
39. **Wendell, K. L., L. Wilson, and M. A. Jordan.** 1993. Mitotic block in HeLa cells by vinblastine: ultrastructural changes in kinetochore-microtubule attachment and in centrosomes. J. Cell Sci. **104:**261–274.
40. **Zirkle, R. E.** 1970. Involvement of the prometaphase kinetochore in prevention of precocious anaphase. J. Cell Biol. **47:**235a.